Research Square

Preprints are preliminary reports that have not undergone peer review.
They should not be considered conclusive, used to inform clinical practice,
or referenced by the media as validated information.

Valence-dependent synaptic plasticity drives approach and avoidance behavior in social context

Camilla Bellone

camilla.bellone@unige.ch

Geneva University https://orcid.org/0000-0002-6774-6275

Pedro Espinosa

University of Geneva https://orcid.org/0000-0002-2202-8982

Benoît J. T. Girard

The University of Geneva https://orcid.org/0000-0002-3914-6483

Lorena Jourdain

University of Geneva

Mattia Lucchini

University of Geneva

Federica Campanelli

University of Geneva

valentina Tiriticco

University of Geneva

Article

Keywords:

Posted Date: July 28th, 2025

DOI: https://doi.org/10.21203/rs.3.rs-6992977/v1

License: This work is licensed under a Creative Commons Attribution 4.0 International License.
Read Full License

Additional Declarations:
There is **NO** Competing Interest.

All experimental procedures involving animals were conducted in accordance with the guidelines and regulations of the Swiss Federal Veterinary Office and were approved by the Geneva Cantonal Veterinary Authority.

Title: Valence-dependent synaptic plasticity drives approach and avoidance behavior in social context

Authors: Pedro Espinosa[(1)], Benoit Girard[(1)], Lorena Jourdain[(1)] , Mattia Lucchini[(1)], Federica Campanelli[(1)], Valentina Tiriticco[(1)] and Camilla Bellone[(1)] *

Affiliations: [(1)] University of Geneva, Department of Fundamental Neuroscience; CMU, 1 rue Michel-Servet, 1211, Geneva, Switzerland.

*Corresponding author. Email: Camilla.Bellone@unige.ch

Abstract

Social interactions critically shape future decisions about engaging with or avoiding conspecifics. However, how the valence of previous social experiences translates into adaptive approach or avoidance behaviors remains unclear. Here, we identify a novel circuit from dopamine D1 receptor (D1R)-expressing neurons in the anterior insular cortex (AIC) to D1R-expressing neurons in the lateral nucleus accumbens (LNAc). We show that valence-specific firing frequencies—low-frequency for reward and high-frequency for aversion—induced distinct synaptic plasticity at these synapses.

Imposing aversive-like firing patterns during rewarding interactions disrupts plasticity and subsequent social approach. Finally, we identify mGluR1 signaling as a critical molecular mechanism selectively required for positive-valence learning. Together, our findings elucidate the synaptic and molecular mechanisms by which social valence guides adaptive behavioral decisions, highlighting frequency-dependent plasticity within a single neural circuit as a dynamic regulator of social approach or avoidance.

Introduction

Understanding how individuals navigate social interactions is crucial for survival across species. Central to this process is the ability to distinguish positive from negative experiences—a concept termed social valence[1]. After an initial interaction, the individual assigns a valence to the experience guiding future decisions to approach or avoid the same conspecific. The flexibility in assigning social valence allows individuals to seek interactions that are beneficial and avoid those that are harmful. Computing and updating social valence involves identifying individual, learning from the experience and integrate these insights to shape behavior. The neuronal mechanisms underlying social valence processing are still largely unknown.

Several circuits contribute to valence-guide behaviors, among which, the Nucleus accumbens (NAc) plays an important role in guiding actions toward rewarding stimuli or away from aversive ones[2–5]. Its principal neurons, GABAergic medium spiny neurons (MSNs) expressing dopamine D1 (D1R) or D2 receptors (D2R) show distinct firing patterns depending on stimulus valence. Appetitive stimuli (e.g., sucrose or saccharin) evoke predominantly inhibitory responses, whereas aversive stimuli (e.g., quinine) trigger excitation in a largely nonoverlapping population[6–9]. Only a minor subset of cells responds to both stimuli—and then in opposite directions—revealing innate valence specificity[6]. Despite this general pattern, the traditional view of strict functional segregation—D1R neurons mediating reward-driven approach and D2R neurons driving aversion-related avoidance—has been revised. Emerging evidence indicates that these populations can indeed cooperate rather than oppose each other, jointly influencing behavioral outcomes[10]. Furthermore, the valence encoded by the NAc can vary based on anatomical subregions, such as rostro-caudal or medial-lateral distinctions, further complicating the understanding of valence coding[11,12].

Despite these advances, most studies on NAc valence encoding have employed gustatory, pharmacological, or Pavlovian paradigms rather than naturalistic social interactions. Consequently, how social experiences shape NAc circuitry to influence future social approach or avoidance behaviors remains unclear. Recent studies highlight the anterior insular cortex (AIC) as a critical structure within the social brain network, demonstrating that its activity and modulation by oxytocin are crucial for social affective behavior[13]. Furthermore, projections from the insular cortex to the NAc specifically regulate social approach towards distressed juvenile conspecifics, suggesting this pathway integrates emotional states with social motivation[14].

Here, we identify and characterize a novel neural circuit connecting D1R glutamatergic neurons in the AIC with D1R-MSNs in the lateral NAc (LNAc). We show that this circuit is activated during rewarding and aversive social interactions. Crucially, we demonstrate that AIC neurons signal rewarding and aversive social interactions through distinct firing frequencies, which in turn drive specific forms of synaptic plasticity: low-frequency (1 Hz) stimulation strengthens synapses by increasing the AMPA/NMDA ratio, while high-frequency (10 Hz) stimulation promotes insertion of calcium-permeable AMPA receptors (CP-AMPARs). Imposing aversive-like burst stimulation during a rewarding social interaction alter synaptic plasticity and disrupts subsequent social approach behavior, establishing a causal link between firing patterns, synaptic plasticity, and behavior. Finally, we identify metabotropic glutamate receptor 1 (mGluR1) as critical for the low-frequency-induced, rewarding synaptic plasticity. Our results thus define a frequency-dependent mechanism involving mGluR1, providing key insights into how synaptic plasticity instructs adaptive social decision-making.

Results:

Juvenile and CD1 interactions are classified as rewarding or aversive experiences.

To investigate how social valence influences subsequent behavior, we developed an assay that reliably induces approach or avoidance in mice. In this ethologically relevant paradigm, adult male mice initially encountered either a sex-matched juvenile, typically associated with affiliative behaviors, or an aggressive adult CD1 mouse, known to provoke aversion. An inanimate object served as a neutral control (Fig. 1A). Upon re-exposure in a corridor apparatus, mice showed approach toward juveniles and avoidance of aggressive CD1 adults (Fig. 1 B and C), an effect specific to aggressive encounters (Fig. supp 1 A–C). We quantified interaction dynamics using DeepLabCut [15] to analyze spatial features such as distance and angle between individuals (Fig. Supp 2 A-E). Additionally, manual annotation of individual contact bouts confirmed juveniles elicited predominantly positive interactions, while aggressive CD1 adults elicited negative ones (Fig. 1 D–G). Applying supervised machine learning via SimBA[16] across the entire dataset independently confirmed the rewarding nature of juvenile encounters and the aversive quality of aggressive CD1 interactions (Fig. 1 H-J). To further validate the rewarding and aversive properties of these stimuli, we conducted conditioned place preference tests, which showed that juvenile mice elicited place preference, whereas aggressive CD1 encounters induced place aversion (Fig. supp 3 A-D)

D1-expressing neurons of Lateral NAc shell (LNAc) encoded proximity regardless of the valence.

Given the established role of D1R MSNs in encoding reward-related information and their involvement in shaping motivated behaviors[17] we next sought to determine whether these neurons are selectively engaged during social interactions of opposing valence. To directly assess valence-specific activity at the single-cell level, we used miniature one-photon calcium imaging using head-mounted miniscopes in freely moving mice (Fig. 2A). This approach allowed us to track the activity of individual D1R MSNs across social interactions of opposing valence, providing a higher-resolution view of how these neurons encode and differentiate between rewarding and aversive social experiences. Ca^{2+} transients increased during social experiences independently on the fact that the experience was rewarding or aversive (Fig. 2 B and C). Furthermore, we found that the Ca^{2+} activity increased when social stimuli were in proximity to the experimental mouse or during contacts (Fig. 2 D-F), regardless of the identity of the stimulus and of the contacts (Fig. 2 E, F, fig supp 4 and 5). Notably, 74.6% of neurons exhibited increased activity during rewarding and aversive experiences (Fig. 2G).

Together, these findings indicate that a large proportion of D1 MSNs in the LNAc are broadly recruited during social engagement, independent of valence, suggesting that proximity strongly drive their activity—laying the foundation for further dissection of how valence-specific information is encoded within this population.

AIC-NAc projecting neurons encoded the social context.

We used a neural activity-dependent labeling approach to investigate the inputs that drive D1R-MSN activity during rewarding and aversive social experiences. We injected Fos-cre-ERT2 mice in the LNAc with a retro-AAV-FLEX-tdTomato virus and, four weeks later, exposed the mice to non-social, rewarding, or aversive stimuli for 15 minutes, followed by tamoxifen administration (Fig. 3A). We identified neurons activated in different rostro-caudal subdivisions of the insular cortex (AIC, medial insular cortex - MIC, and posterior insular cortex - PiC) and in the amygdala (Fig. 3 B, C). The insular cortex has an integrative function, plays an essential role in salience processing and attention, and gates executive control[18]. These functions are implicated in social behavior and valence processing[19,20]. Retrograde rabies tracing from the LNAc revealed that monosynaptic input to lateral D1R-MSNs originates exclusively from the anterior insula. (fig. supp 6, A-E). To identify the socially active neurons in the AIC that project to the LNAc, we next used RNA scope in situ hybridization to double label c-Fos and Drd1 mRNA. We observed that 88.16% of juvenile-activated neurons and 81.4% of CD1-activated neurons were Drd1-positive (Fig. 3D). We confirmed these results using a bicolor virus approach, injecting AAVrg-ef1a-DO-DIOTdTomato-eGFP in the LNAc and labeling neurons in the AIC (Fig. 3 E-G). We reveal in the AIC a higher proportion of D1R-positive neurons projecting to the LNAc.

AIC to LNAc D1R neurons encode valence

Next, we examined Ca^{2+} activity in D1R-positive AIC neurons projecting to the LNAc during rewarding and aversive social interactions using miniscopes (Fig. 4A). We observed increased Ca^{2+} signals in these neurons during both rewarding and aversive conditions (Fig. 4 B, C). Specifically, AIC→LNAc neurons showed elevated activity during positive and negative social contacts, independently of proximity (Fig. 4, D–F, Fig. supp. 7 and 8), suggesting that their activity primarily encodes social interaction rather than distance. Additionally, we found a substantial overlap (67.5%) of neurons active across both types of social experiences (Fig.

4G). These results indicate that AIC→LNAc neurons robustly encode social interactions, irrespective of valence, positioning them as key players in processing social information.

Valence-dependent synaptic plasticity at AIC to LNAc synapses

Given that mice adapt their behavior based on previous social experiences (Fig. 1A, supp Fig. 1–3) and that D1R neurons in the AIC projecting to the LNAc are activated by interactions of both positive and negative valence, we investigated whether these social encounters leave lasting changes at AIC-to-LNAc synapses. Synaptic plasticity is widely recognized as a cellular mechanism underlying learning, and AMPA receptor-mediated transmission has been specifically linked to adaptive behavioral modifications[21–25]. We therefore hypothesized that rewarding and aversive social interactions would induce distinct forms of plasticity at these synapses.

To test this hypothesis, we first confirmed the specificity of projections from D1R-expressing AIC neurons onto D1-MSNs in the LNAc. Using a dual-virus approach in D1-Cre mice, injection of ChR2-containing virus in D1R-AIC and mCherry virus in D1R-LNAc, we performed paired whole-cell recordings from identified D1R-positive and D1R-negative neurons in the LNAc. We found that excitatory inputs from the AIC specifically targeted D1R-MSNs (Fig. Supp 9), thus defining the cellular basis for a selective, top-down circuit.

We next assessed synaptic function 24 hours after social experiences by performing whole-cell recordings from D1R-MSNs in mice previously exposed to either rewarding or aversive conspecifics. We measured the AMPA/NMDA ratio as an indicator of synaptic strength and evaluated the rectification index to detect the presence of calcium-permeable AMPA receptors (CP-AMPARs)[26], a signature associated with aversive learning. Rewarding interactions selectively increased the AMPA/NMDA ratio, whereas aversive experiences specifically enhanced AMPAR rectification (Fig. 5, D and E). These findings indicate that distinct forms of synaptic plasticity are induced by the valence of social encounters and are restricted to D1-positive MSNs, as neither form of plasticity was observed in neighboring D1-negative neurons or following non-social rewarding or aversive experiences (Fig. supp 10-11).

Frequency-Specific AIC Firing Drives Valence-Dependent NAc Plasticity

To explain how distinct forms of synaptic plasticity can arise from experiences of opposite valence, we hypothesized that differences in neuronal firing patterns might encode valence-specific information. To test this, we first analyzed calcium signals measured with miniscopes

from D1R-MSN in the LNAc and LNAc-projecting AIC neurons using Fast Fourier Transform (FFT). Using this approach, we observed no frequency differences in LNAc D1R-MSN activity between rewarding and aversive interactions (supp Fig 12 A–D), suggesting these neurons signal social engagement rather than valence. In contrast, calcium signals from AIC→LNAc neurons showed a shift toward higher frequencies during aversive interactions compared to rewarding ones (supp Fig 12 E–H). In vivo single-unit recordings confirmed that this shift corresponds to increased burst firing during aversive interactions (supp Fig 14 A-E). Additionally, a classifier trained on spike patterns accurately distinguished rewarding from aversive experiences with high accuracy (>80%, supp Fig 14 F-G). Thus, aversive encounters selectively enhance burst firing in AIC→LNAc neurons, creating a frequency-specific code capable of driving valence-dependent plasticity downstream in the NAc.

To test whether the shifts in firing patterns observed in vivo are sufficient to drive the distinct forms of synaptic plasticity induced by rewarding and aversive interactions, we applied stimulation protocols that mimic these changes, based on widely used approaches to induce plasticity in the NAc [27,28]

To test whether firing patterns observed in vivo drive the distinct forms of synaptic plasticity induced by rewarding and aversive interactions, we next used stimulation protocols that replicate these frequencies in slices. In acute slices, we found both 1 Hz and 10 Hz stimulation decreased the amplitude of AMPAR-EPCSc measured at -70mV (Fig. 6 A, B). Interestingly, these forms of LTD were accompanied by different expression mechanisms. When we look at the consequence of LTD 1 hour after the stimulation protocol, we observed that tonic 1 Hz stimulation of AIC→NAc terminals specifically increased the AMPA/NMDA ratio, whereas burst-patterned 10 Hz stimulation—reflecting aversive-like firing—induced calcium-permeable AMPA receptor (CP-AMPAR) insertion and enhanced rectification with no changes in Pair Pulse Ratio (Fig. 6 C-D).

Finally, we investigated whether the synaptic changes induced by distinct firing patterns are stable and long-lasting in vivo. Based on our second exposure protocol, we hypothesized that if a form of learning occurred, it would leave a trace in the form of persistent synaptic plasticity observable 24 hours later. To test this, we expressed ChR2 in D1R-MSNs, implanted bilateral optic fibers above the NAc, and delivered unilateral optogenetic in vivo stimulation at 1 Hz or 10 Hz. Twenty-four hours later, ex vivo recordings confirmed that 1 Hz stimulation increased the AMPA/NMDA ratio, whereas 10 Hz stimulation enhanced rectification compared to the ipsilaterally stimulated control (Fig. 6 E–G). Together, these

results demonstrate that frequency-specific firing patterns from AIC neurons are sufficient to drive long-lasting, valence-dependent synaptic plasticity in the NAc, providing a direct link between AIC firing dynamics and the synaptic modifications underlying approach and avoidance behaviors.

Valence-dependent synaptic plasticity controls subsequent approach behavior.

We next tested whether imposing the aversive-like 10 Hz burst pattern onto AIC→LNAc terminals during a naturally rewarding interaction could reverse both synaptic plasticity and approach behavior (Fig. 7A-C). Experimental mice freely interacted with juvenile conspecifics while we delivered optogenetic 10 Hz bursts to AIC terminals specifically during interaction contacts. Control mice underwent identical interactions without light stimulation. Importantly, light delivery alone did not alter interaction time (supp Fig 14). Twenty-four hours later, in the approach/avoidance test, controls showed a strong preference for the juvenile, whereas mice that experienced the 10 Hz stimulation no longer displayed approach behavior (Fig 7 D-E). These results indicate that aversive-like burst firing imposed during a rewarding social interaction can neutralize the positive valence of the encounter.
To investigate the causal link between the synaptic changes and the behavioral reversal, we performed whole-cell recordings from D1-MSNs. In control mice, the AMPA/NMDA ratio at AIC→LNAc synapses remained elevated, consistent with the rewarding nature of juvenile interactions. In contrast, mice receiving the aversive-like 10 Hz stimulation showed a significantly reduced AMPA/NMDA ratio (Fig. 7F), like the profile normally seen after aversive interactions. Although the rectification index did not differ between groups, it correlated linearly with the avoidance index (Fig. 7 G-H), indicating that the degree of calcium-permeable AMPAR insertion directly predicts subsequent social avoidance.
Together, these findings show that imposing aversive-like firing patterns onto AIC terminals during a rewarding social encounter overrides the natural plasticity, abolishing subsequent approach behavior. This establishes a direct causal link between AIC firing patterns, synaptic plasticity, and adaptive social decision-making

Positive social valence requires mGluR1 signalling

The observation that aversive-like 10 Hz bursts can suppress the increase in AMPA/NMDA induced by rewarding juvenile encounters suggests that distinct firing frequencies recruit

separate molecular mechanisms at AIC→LNAc synapses. Metabotropic glutamate receptors, particularly mGluR1, are known modulators of synaptic plasticity in the NAc. Therefore, we asked whether mGluR1 specifically control valence-dependent plasticity. We locally deleted mGluR1 in the LNAc by bilaterally injecting AAV-Cre into mGluR1-knockout (mGluR1-KO) mice (controls received AAV-GFP; Fig. 8A). In the approach/avoidance assay, mGluR1-KO mice did not develop a preference for juveniles but continued to avoid aggressive CD1 mice (Fig. 8, B–E). This indicates a specific impairment of positive, but not negative, valence learning.

Consistent with this behavioral phenotype, whole-cell recordings from MSNs showed that deletion of mGluR1 did not alter the AMPA/NMDA ratio compared to controls yet significantly increased the rectification index (Fig. 8F). This synaptic profile indicates a default shift toward an aversion-like state, characterized by enhanced insertion of calcium-permeable AMPARs. Together, these data show that mGluR1 acts as a molecular gate required for rewarding, low-frequency-induced plasticity. Its absence biases the circuit toward aversive plasticity.

Discussion

In this study, we characterize a novel circuit linking D1R neurons in the AIC with D1R neurons in the LNAc, active during both positive (juvenile) and negative (aggressive) social interactions. We demonstrate that AIC neurons signal social valence through distinct firing frequencies, driving specific forms of synaptic plasticity: low-frequency stimulation increases the AMPA/NMDA ratio, while high-frequency stimulation inserts calcium-permeable AMPA receptors.

The affective valence of a stimulus—the sense that something is “good” or “bad”—has both hedonic (pleasurable vs. unpleasant) and motivational (approach-promoting vs. avoidance-promoting) dimensions[29]. Our data show that social cues (contact with a conspecific) can acquire either positive or negative valence and thereby bias mice toward approach or avoidance. Such flexibility is adaptive: individuals must rapidly distinguish friends from foes and update those assignments as circumstances change.

How is this flexibility implemented in the brain? Two broad frameworks have been proposed. The “affective-modules” view posits hard-wired circuits dedicated to either positive or negative valence. In contrast, the “affective-modes” hypothesis argues that a single neural

module can adopt multiple affective states, its output shifting with neurochemical milieu, firing pattern, or network context [29].

Our findings align strongly with the affective-modes account. Within one anatomically defined pathway—D1R neurons in the AIC projecting to D1R MSNs in LNAc—social encounters of opposite valence elicit distinct firing frequencies. These frequencies, in turn, drive opposite forms of synaptic plasticity (AMPA/NMDA potentiation vs. CP-AMPAR insertion) that predict future approach or avoidance. Thus, valence is not hard-wired into separate circuits but dynamically encoded by the plastic state of a single circuit, which can switch between "reward" and "aversion" modes.

Together, these results extend classic limbic theories of valence by demonstrating that frequency-dependent plasticity within a flexible affective mode, rather than fixed circuitry, underlies adaptive social decision-making.

The idea that the NAc might contain dedicated regions for processing either positive (rewarding) or negative (aversive) experiences has evolved considerably over the last years. Classic views suggested that certain subregions or neuronal populations—such as D1R or D2R neurons—might consistently mediate positive or negative experiences[30,31]. However, more recent work supports an "affective modes" framework, proposing that these neuronal populations are not permanently tied to one valence but can shift roles depending on the context[29].

Our findings further refine this framework. Specifically, we observed that the very same neurons in the D1R-expressing neurons in the LNAc become active during both positive and negative interactions. Remarkably, what differentiates these positive versus negative experiences is not the identity of the activated neurons, but rather the nature of the synaptic changes occurring at their connections with the AIC.

We found that during interactions with juvenile mice, AIC neurons fire at low frequency, inducing a form of synaptic plasticity that promotes approach behavior during subsequent encounters. In contrast, during aggressive interactions, AIC projections to the LNAc fire at higher frequencies, triggering a different type of plasticity that facilitates avoidance learning. Thus, the emotional valence of social interactions appears to be determined at the synaptic rather than neuronal level. Several critical questions remain open for future investigation. Future studies should examine precisely how these synaptic changes translate into different firing patterns of NAc neurons and how these patterns influence subsequent behavioral decisions. Additionally, investigating which downstream brain regions receive signals from these NAc neurons to generate approach or avoidance behaviors will be crucial. These future

experiments will deepen our understanding of how synaptic plasticity within fixed neural circuits dynamically shapes social behavior.

Our results extend the understanding of synaptic plasticity mechanisms regulated by Group I mGluRs within the NAc, particularly emphasizing the role of mGluR1 in encoding social valence. Previous studies have established that activation of Group I mGluRs in the NAc induces long-term depression (LTD) of excitatory synapses through retrograde endocannabinoid signaling and internalization of AMPA receptors[32–34]. Moreover, increasing mGluR signaling pharmacologically via positive allosteric modulators has demonstrated potential in attenuating drug-seeking behaviors and reversing drug-induced physiological changes[35,36]. Notably, synapse-specific roles have emerged, with distinct subtypes selectively regulating particular afferents—mGluR1 predominantly modulating prefrontal cortex -to-NAc synapses and mGluR5 governing midline thalamic-to-NAc synapses[28].

Aligned with these observations, we found that selective downregulation of mGluR1 in the lateral NAc (LNAc) impairs learning to approach positive social cues without disrupting avoidance learning, indicating a unique role of mGluR1 signaling in positively-valenced motivational encoding. Intriguingly, this prompts the open question of which synaptic mechanisms or molecular pathways specifically underpin avoidance learning, given their apparent independence from mGluR1 signaling in our model. Moreover, the baseline inward rectification we observed at AIC-to-LNAc D1R synapses—typically indicative of calcium-permeable AMPA receptor (CP-AMPAR) enrichment—raises intriguing questions about the specific function of mGluR1 at these versus other synaptic connections within the NAc. Given the known role of mGluR1 in mediating CP-AMPAR removal after drug exposure, it will be important for future studies to explore whether mGluR1 differentially regulates AMPAR subunit composition and synaptic plasticity at distinct NAc inputs. Collectively, these data highlight the necessity for synapse-specific analyses and underscore the potential of targeting mGluR1 signaling pathways for therapeutic modulation of motivational disorders.

References

1. Padilla-Coreano, N., Tye, K. M. & Zelikowsky, M. Dynamic influences on the neural encoding of social valence. *Nat Rev Neurosci* 23, 535–550 (2022).
2. Ray, M. H., Moaddab, M. & McDannald, M. A. Threat and Bidirectional Valence Signaling in the Nucleus Accumbens Core. *The Journal of Neuroscience* 42, 817–833 (2022).
3. Klawonn, A. M. & Malenka, R. C. Nucleus Accumbens Modulation in Reward and Aversion. *Cold Spring Harb Symp Quant Biol* 83, 119–129 (2018).
4. Baldo, B. A. & Kelley, A. E. Discrete neurochemical coding of distinguishable motivational processes: insights from nucleus accumbens control of feeding. *Psychopharmacology (Berl)* 191, 439–459 (2007).
5. Vieitas-Gaspar, N., Soares-Cunha, C. & Rodrigues, A. J. From valence encoding to motivated behavior: A focus on the nucleus accumbens circuitry. *Neurosci Biobehav Rev* 172, 106125 (2025).
6. Roitman, M. F., Wheeler, R. A. & Carelli, R. M. Nucleus Accumbens Neurons Are Innately Tuned for Rewarding and Aversive Taste Stimuli, Encode Their Predictors, and Are Linked to Motor Output. *Neuron* 45, 587–597 (2005).
7. Wilson, D. I. G. & Bowman, E. M. Nucleus accumbens neurons in the rat exhibit differential activity to conditioned reinforcers and primary reinforcers within a second-order schedule of saccharin reinforcement. *European Journal of Neuroscience* 20, 2777–2788 (2004).
8. Nicola, S. M., Yun, I. A., Wakabayashi, K. T. & Fields, H. L. Firing of Nucleus Accumbens Neurons During the Consummatory Phase of a Discriminative Stimulus Task Depends on Previous Reward Predictive Cues. *J Neurophysiol* 91, 1866–1882 (2004).
9. Gerfen, C. R. The neostriatal mosaic: multiple levels of compartmental organization. in *Advances in Neuroscience and Schizophrenia* 43–59 (Springer Vienna, Vienna, 1992). doi:10.1007/978-3-7091-9211-5_4.
10. Steinberg, E. E. *et al.* Positive Reinforcement Mediated by Midbrain Dopamine Neurons Requires D1 and D2 Receptor Activation in the Nucleus Accumbens. *PLoS One* 9, e94771 (2014).
11. Chen, G. *et al.* Distinct reward processing by subregions of the nucleus accumbens. *Cell Rep* 42, 112069 (2023).
12. Baldo, B. A., Sadeghian, K., Basso, A. M. & Kelley, A. E. Effects of selective dopamine D1 or D2 receptor blockade within nucleus accumbens subregions on ingestive behavior and associated motor activity. *Behavioural Brain Research* 137, 165–177 (2002).
13. Rogers-Carter, M. M. *et al.* Insular cortex mediates approach and avoidance responses to social affective stimuli. *Nat Neurosci* 21, (2018).
14. Rogers-Carter, M. M., Djerdjaj, A., Gribbons, K. B., Varela, J. A. & Christianson, J. P. Insular Cortex Projections to Nucleus Accumbens Core Mediate Social Approach to Stressed Juvenile Rats. *The Journal of Neuroscience* 39, (2019).
15. Mathis, A. *et al.* DeepLabCut: markerless pose estimation of user-defined body parts with deep learning. *Nat Neurosci* 21, 1281–1289 (2018).
16. Goodwin, N. L. *et al.* Simple Behavioral Analysis (SimBA) as a platform for explainable machine learning in behavioral neuroscience. *Nat Neurosci* (2024) doi:10.1038/s41593-024-01649-9.
17. Gunaydin, L. A. *et al.* Natural Neural Projection Dynamics Underlying Social Behavior. *Cell* 157, (2014).

18. Gogolla, N. The insular cortex. *Current Biology* 27, (2017).
19. Gehrlach, D. A. *et al.* Aversive state processing in the posterior insular cortex. *Nat Neurosci* 22, 1424–1437 (2019).
20. Miura, I. *et al.* Encoding of social exploration by neural ensembles in the insular cortex. *PLoS Biol* 18, e3000584 (2020).
21. Clem, R. L. & Huganir, R. L. Calcium-Permeable AMPA Receptor Dynamics Mediate Fear Memory Erasure. *Science (1979)* 330, 1108–1112 (2010).
22. Tye, K. M., Stuber, G. D., de Ridder, B., Bonci, A. & Janak, P. H. Rapid strengthening of thalamo-amygdala synapses mediates cue–reward learning. *Nature* 453, 1253–1257 (2008).
23. Rumpel, S., LeDoux, J., Zador, A. & Malinow, R. Postsynaptic Receptor Trafficking Underlying a Form of Associative Learning. *Science (1979)* 308, 83–88 (2005).
24. Rogan, M. T., Stäubli, U. V. & LeDoux, J. E. Fear conditioning induces associative long-term potentiation in the amygdala. *Nature* 390, 604–607 (1997).
25. McKernan, M. G. & Shinnick-Gallagher, P. Fear conditioning induces a lasting potentiation of synaptic currents in vitro. *Nature* 390, 607–611 (1997).
26. Bellone, C. & Lüscher, C. Cocaine triggered AMPA receptor redistribution is reversed in vivo by mGluR-dependent long-term depression. *Nat Neurosci* 9, 636–641 (2006).
27. Pascoli, V. *et al.* Contrasting forms of cocaine-evoked plasticity control components of relapse. *Nature* 509, (2014).
28. Turner, B. D., Rook, J. M., Lindsley, C. W., Conn, P. J. & Grueter, B. A. mGlu1 and mGlu5 modulate distinct excitatory inputs to the nucleus accumbens shell. *Neuropsychopharmacology* 43, 2075–2082 (2018).
29. Berridge, K. C. Affective valence in the brain: modules or modes? *Nat Rev Neurosci* 20, 225–234 (2019).
30. Soares-Cunha, C. *et al.* Activation of D2 dopamine receptor-expressing neurons in the nucleus accumbens increases motivation. *Nat Commun* 7, 11829 (2016).
31. Cole, S. L., Robinson, M. J. F. & Berridge, K. C. Optogenetic self-stimulation in the nucleus accumbens: D1 reward versus D2 ambivalence. *PLoS One* 13, e0207694 (2018).
32. Loweth, J. A. *et al.* Synaptic depression via mGluR1 positive allosteric modulation suppresses cue-induced cocaine craving. *Nat Neurosci* 17, 73–80 (2014).
33. McCutcheon, J. E. *et al.* Group I mGluR Activation Reverses Cocaine-Induced Accumulation of Calcium-Permeable AMPA Receptors in Nucleus Accumbens Synapses via a Protein Kinase C-Dependent Mechanism. *The Journal of Neuroscience* 31, 14536–14541 (2011).
34. Robbe, D., Kopf, M., Remaury, A., Bockaert, J. & Manzoni, O. J. Endogenous cannabinoids mediate long-term synaptic depression in the nucleus accumbens. *Proceedings of the National Academy of Sciences* 99, 8384–8388 (2002).
35. Grueter, B. A., McElligott, Z. A., Robison, A. J., Mathews, G. C. & Winder, D. G. *In Vivo* Metabotropic Glutamate Receptor 5 (mGluR5) Antagonism Prevents Cocaine-Induced Disruption of Postsynaptically Maintained mGluR5-Dependent Long-Term Depression. *The Journal of Neuroscience* 28, 9261–9270 (2008).
36. Loweth, J. A., Tseng, K. Y. & Wolf, M. E. Adaptations in AMPA receptor transmission in the nucleus accumbens contributing to incubation of cocaine craving. *Neuropharmacology* 76, 287–300 (2014).

Acknowledgments: We thank Giuseppe Chindemi for his support with data analysis, which, despite its value, could not be included in the final version of this publication. We are also grateful to Christian Lüscher and Tinaig Le Borgne for his insightful suggestions on the manuscript, and to Lucy Mohrhauer for her assistance with Supplementary Figure 2.. **Funding:** P.E. was supported by the Swiss Government Excellence Scholarship (FCS) for PhD Studies Grant ESKAS-Nr: 2017.0922. C.B. is supported by the Swiss National Science Foundation and by the ERC SocialNac. **Author Contributions:** P.E. and C.B. conceived the project and wrote the manuscript. P.E. performed all experiments. L.J. provided assistance with all experimental procedures. F.C. contributed to the patch-clamp recordings. B.G. conducted the analyses using DeepLabCut (DLC), SimBA, and in vivo electrophysiology. Anatomical tracing experiments were carried out by P.E. with assistance from M.L. Manual cell counting was performed by M.L. and V.T. Data analysis and statistical evaluations were performed by P.E. All figures were prepared by P.E. **Competing interests:** The authors declare no competing interests. **Data and materials availability**: Scripts and raw data will be uploaded to a server to grant access to them.

Figures

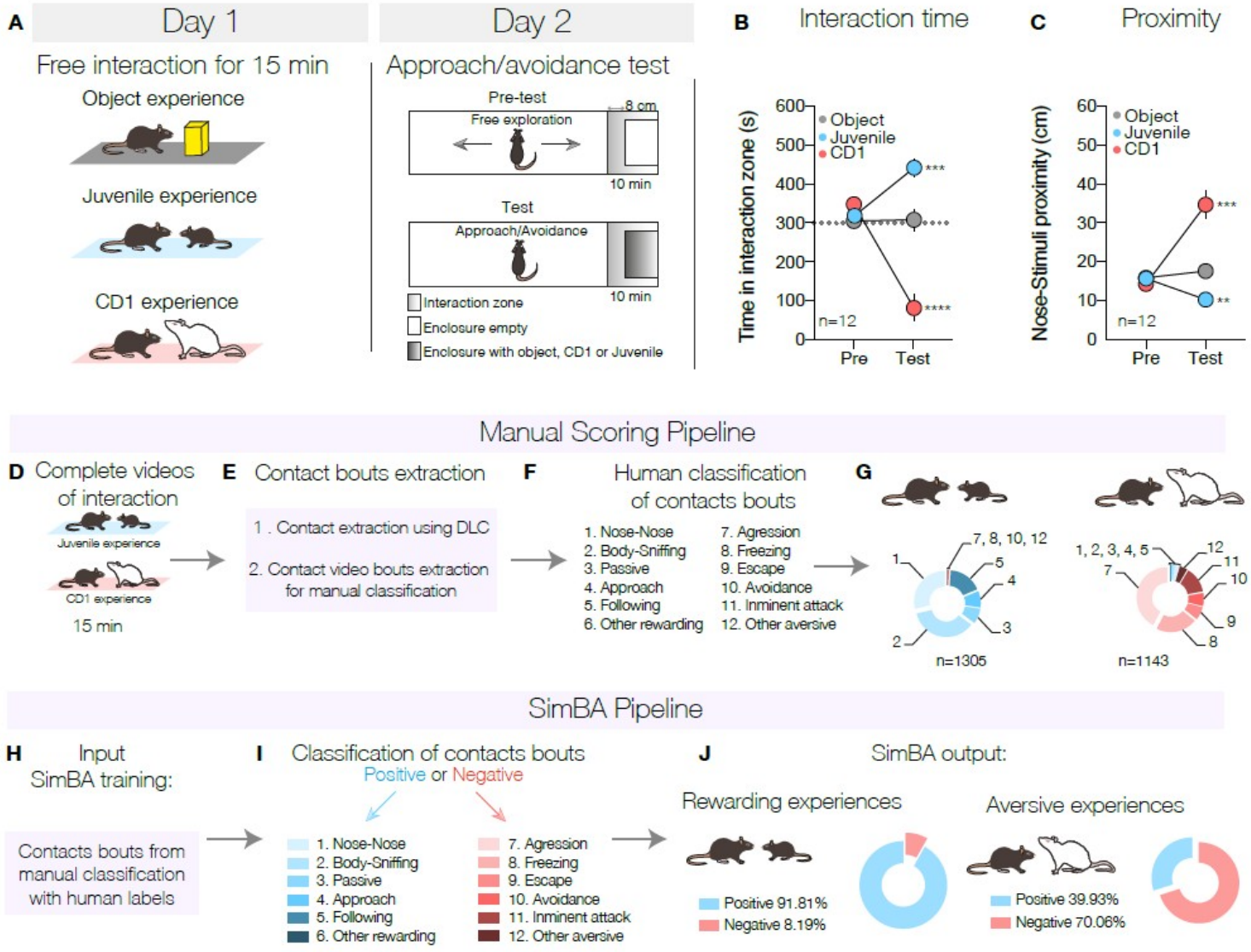


Figure 1

Juvenile and CD1 experiences induce learned approach and avoidance behavior. (A) Mice were exposed to an object, a juvenile, or CD1 mice for a 15-minute period of free social interaction. After 24 hours, the animals were placed in a new arena where, following 10 minutes of free exploration with an empty enclosure, an enclosure containing the stimuli from the previous day was introduced. (B) Time spent in the interaction zone on day 2, with *** indicating $p = 0.0002$, **** denoting $p < 0.0001$, and $p = 0.9130$ for interactions with the object. (C) Proximity to the stimulus mouse on day 2, measured as the distance between the mouse's nose point and the center of the enclosure; ** indicates $p = 0.0013$, *** represents $p = 0.0001$, and $p = 0.3020$ for the object. (D-G) Schematics showing how we manual label the contacts and their subsequent quantification. (H-I) Classification of contacts into positive and negative categories in preparation for training SimBA. (J) Classification of contacts by SimBA.

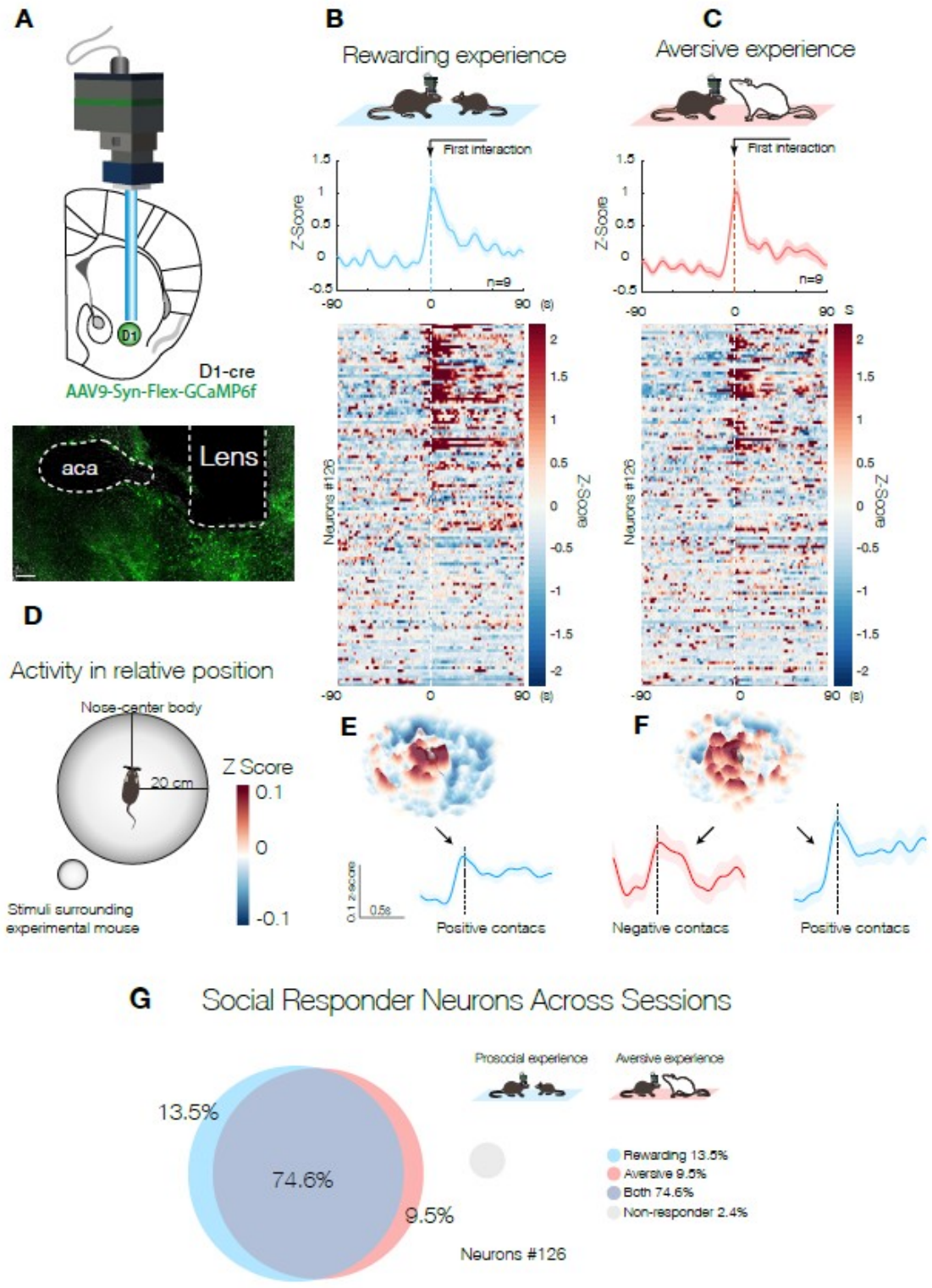


Figure 2

D1-MSNs encode proximity to social stimuli, independent of experience valence. (A) Schematic of injection and implantation sites (Scale 250uM). (B) Average activity during a rewarding experience aligned with the first interaction. The heatmap represents the activity of individual neurons (each row represents one neuron). (C) Average activity during an aversive experience aligned with the first interaction. The heatmap represents the activity of individual neurons (each row represents one neuron).

(D) Schematic of a 3D heatmap representing the calcium activity in position relative to the stimuli. (E) Heatmap showing the activity in positions relative to juvenile stimuli. (F) Heatmap showing the activity in positions relative to CD1 stimuli. (G) Proportion of neurons that respond to social stimuli.

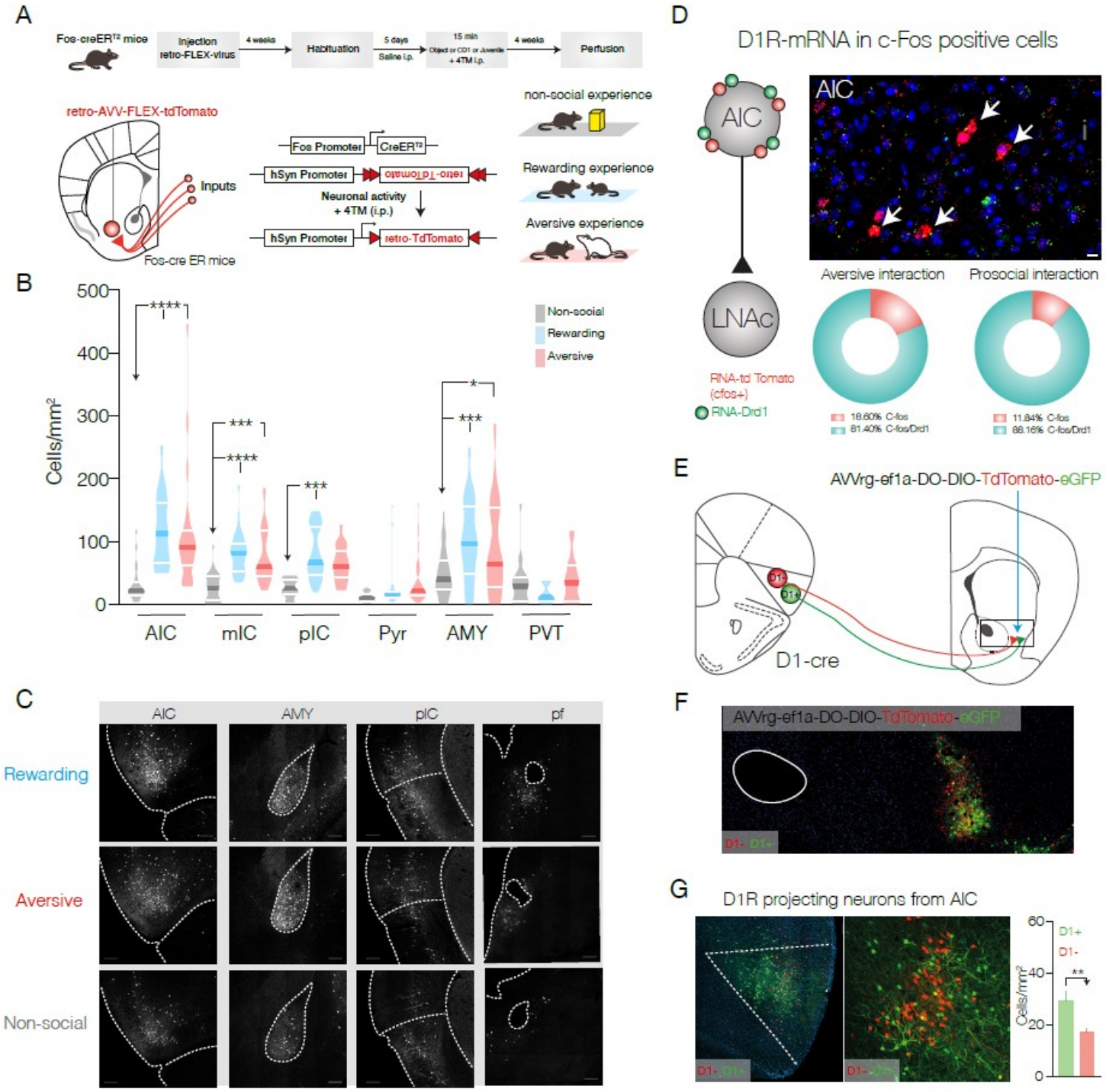


Figure 3

Characterization of AIC-LNAc pathway. (A) Schema of the experimental protocol showing viral injection and transgenic construct activation by 4-OH tamoxifen. (B) Quantification of cell densities from the main brain regions projecting to the LNAc, representing the overall active inputs during free social

interaction. (C) Representative pictures of active neurons in various brain regions. One-way ANOVA was used as the statistical test, with the following significance levels: AIC: ****p<0.0001, mIC: ****p<0.0001, ***p=0.0002, pIC: ***p=0.0001. AMY: *p=0.0378, ***p=0.0004. n=4 per condition (prosocial, aversive, non-social). (D) In situ hybridization for mRNA of D1R and td-Tomato, showing high correspondence between c-fos positive cells (mRNA td-Tomato) and D1R mRNA (scale: 10 μm). n=2 for aversive and n=3 for rewarding experience. Most neurons colocalize for mRNA of td-tomato (c-fos signal) and D1R. (E) Schematic of viral injection using a bicolor retrovirus that turns green in the presence of cre-recombinase and remains red without it (scale: 500 μm). Below, the representative picture of the injection site (F). (G) Representative image from AIC illustrating the D1R projecting neuron subpopulation. The left picture shows AIC with D1 positive neurons in green and D1 negative in red. The right shows a magnified view of AIC detailing the proportion of D1 positive and negative cells. Right panel, Histogram represents the quantification of D1 positive and negative cells in AIC, using an unpaired t-test, with **p=0.0091, n=4.

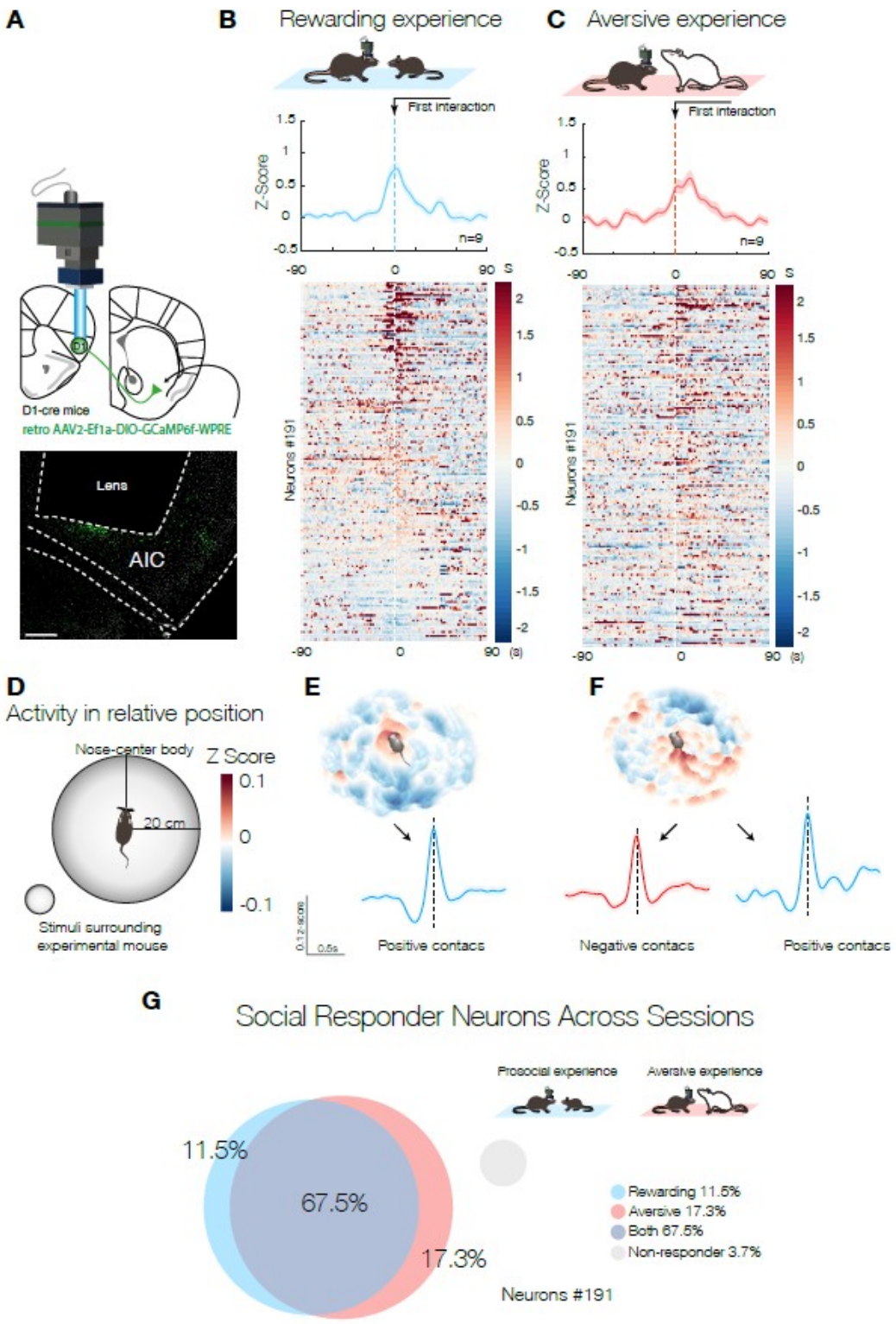


Figure 4

D1R-AIC neurons predicts social valence. (A) Schematic of injection and implantation sites. (B) Average activity during a rewarding experience aligned with the first interaction. The heatmap represents the activity of individual neurons (each row represents one neuron). (C) Average activity during an aversive experience aligned with the first interaction. The heatmap represents the activity of individual neurons (each row represents one neuron). (D) Schematic of a 3D heatmap representing the calcium

activity in position relative to the stimuli. (E) Heatmap showing the activity in positions relative to juvenile stimuli. (F) Heatmap showing the activity in positions relative to CD1 stimuli. (G) Proportion of neurons that respond to social stimuli.

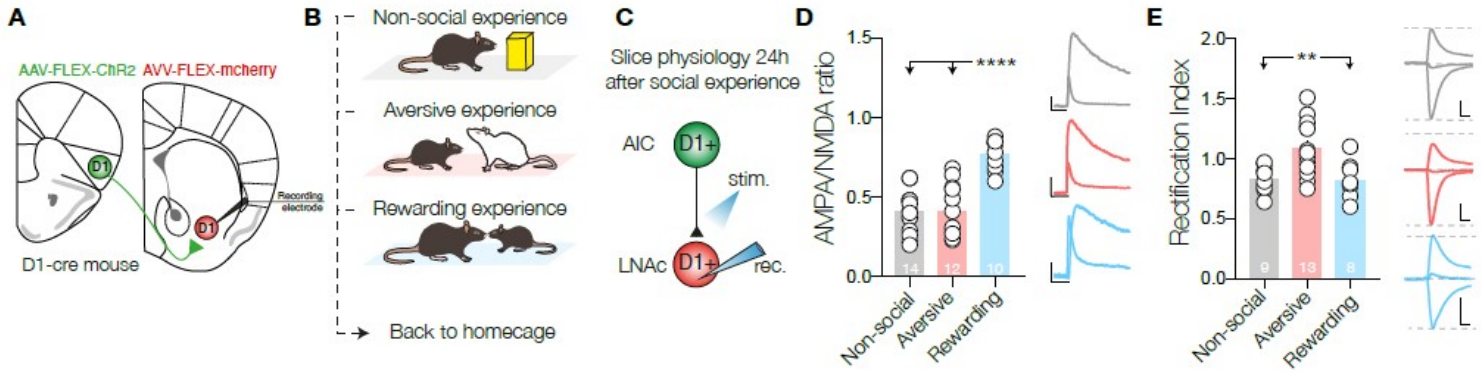


Figure 5

Social valence induce specific long-term synaptic plasticity in AIC-LNAc pathway. (A) Schematic representation of viral injection into the Lateral Nucleus Accumbens (LNAc) and Anterior Insular Cortex (AIC). (B) Diagrammatic representation of the behavioral paradigm. (C) Schematic of patch-clam whole cell recording protocol. (D) Bar graph showing the AMPA/NMDA ratio 24 hours post-behavioral experiment; to the right are example traces, with **** indicating $p < 0.0001$. (E) Bar graph showing the rectification index 24 hours after free interaction; to the right are example traces, with ** denoting $p = 0.0094$ for Aversive vs. Prosocial and ** for Aversive vs. Object $p = 0.0077$.

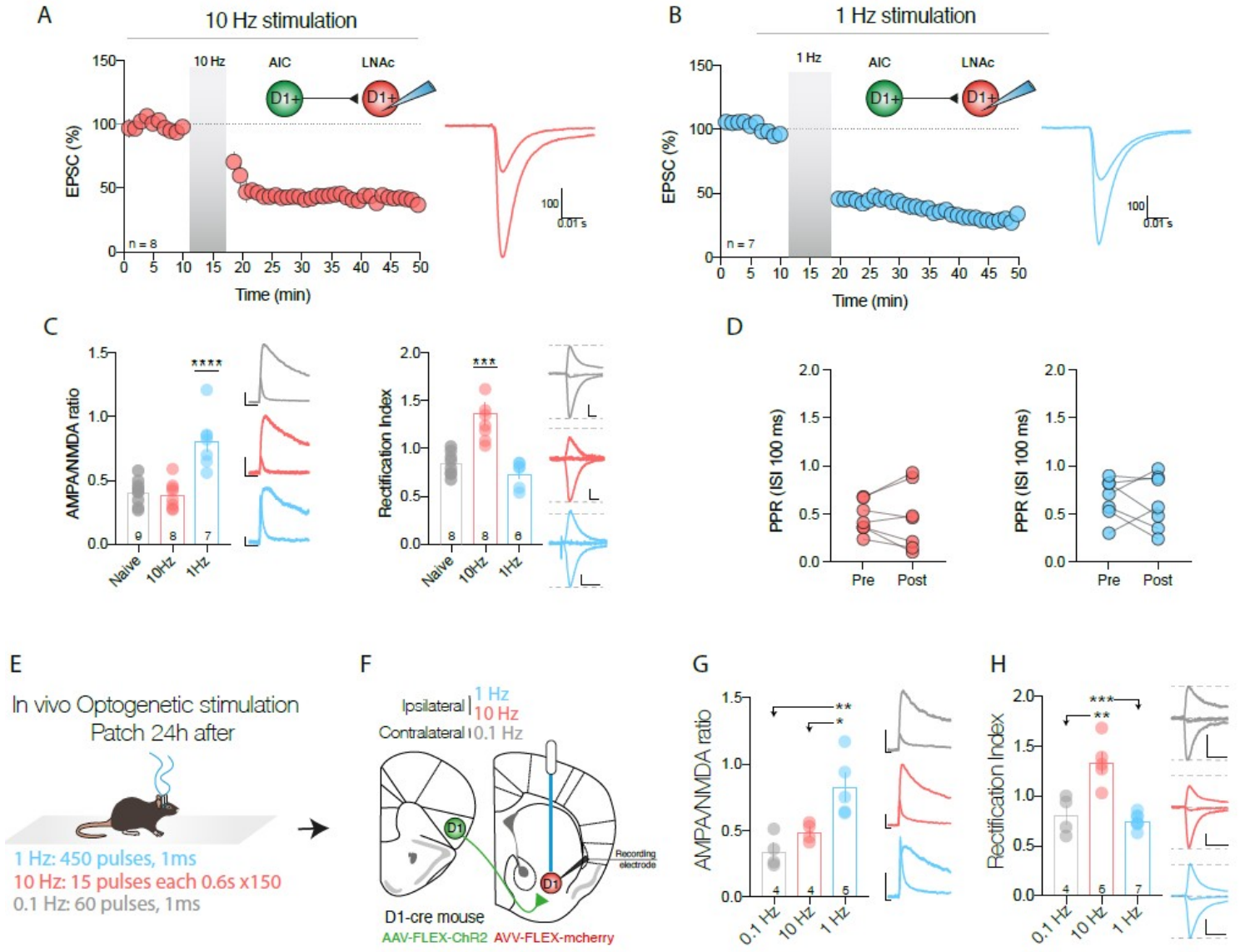


Figure 6

Valence-dependent synaptic plasticity in the AIC → LNAc pathway is frequency-specific (A, B) Time course of optically evoked EPSC amplitudes recorded from D1-positive AIC-to-LNAc synapses in acute slices (whole-cell voltage clamp, −70 mV). 10 Hz (A) or 1 Hz (B) trains (gray bar) produced a long-lasting depression (LTD). (C) Summary of the AMPA/NMDA (A/N) ratio after each stimulation protocol. Representative AMPA (−70 mV) and NMDA (+40 mV) traces are shown on the right. **** $p < 0.0001$, one-way ANOVA. (D) Rectification index (RI) for the groups in C, derived from I–V plots; example traces are shown on the right. *** $p \leq 0.0005$. (E) Paired-pulse ratio (PPR, 100 ms inter-stimulus interval) before (Pre) and after (Post) the in-slice plasticity induction in the same cells shown in A-B. (F) Schematic of the in-vivo optogenetic protocol. In the ipsilateral hemisphere, AIC terminals in the LNAc received either 10 Hz or 1 Hz stimulation; the contralateral hemisphere received only 0.1 Hz test pulses. (G) Viral strategy and fibre placements: AAV-DIO-ChR2-eYFP injected into AIC of D1-Cre mice; optic fibres implanted above the LNAc. (H) AMPA/NMDA ratio measured ex-vivo 24 h after the in-vivo stimulation. ** $p = 0.0036$; * $p = 0.0292$; one-way ANOVA. (I) Rectification index 24 h after in-vivo stimulation. ** $p = 0.0011$; *** $p =$

0.0001; one-way ANOVA. Numbers in bars denote individual cells. Data are mean ± SEM. Scale bars: 50 pA, 10 ms.

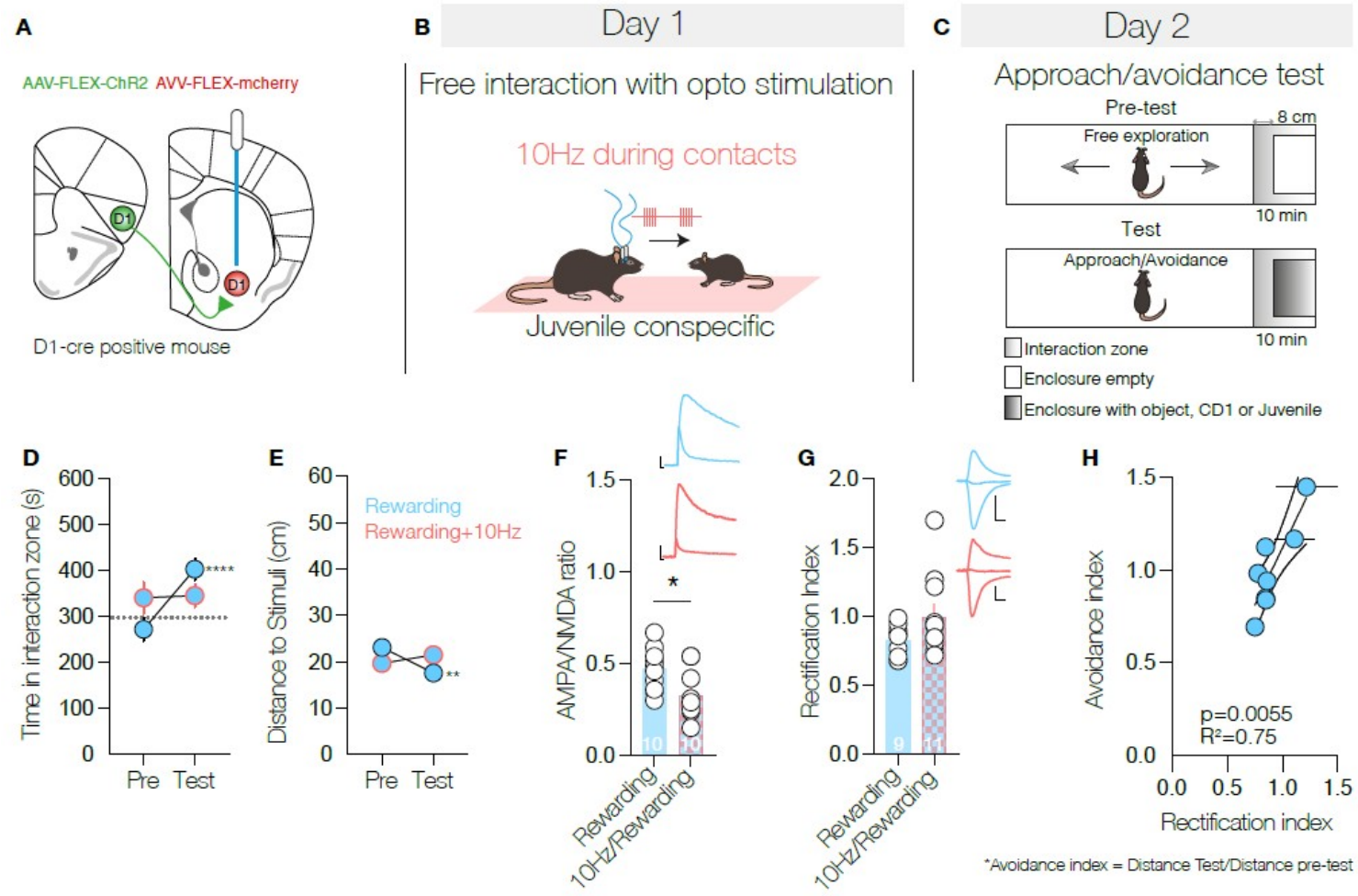


Figure 7

Valence-dependent synaptic plasticity is essential for learned approach behavior. (A) Schematic indicating the site of viral injection and placement of the optical fiber. (B) Diagram detailing the protocol, and the delivery of 10Hz optical stimulation during bouts of contact. (C) On Day 2, animals were placed in a new arena and, after 10 minutes of free exploration with an empty enclosure, were introduced to an enclosure containing the stimuli from the previous day. (D) Graph depicting the duration of interaction within the zone, with **** signifying $p < 0.0001$ for animals that did not receive the stimulation and $p = 0.8745$ for animals that received the 10Hz stimulation. (E) Graph depicting the distance to stimuli, with ** indicating $p = 0.0027$ and $p = 0.4030$ for rewarding experiences with 10Hz stimulation. (F) Bar graph showing the AMPA/NMDA ratio, with * indicating $p = 0.020$. (G) Bar graph showing the rectification index, $p = 0.1048$. (H) A correlation graph between the rectification index and the avoidance index, calculated as the distance during the post-test divided by the distance during the pre-test, with $p = 0.0055$ and $R^2 = 0.75$ (each dot represents a single animal, $n = 8$). A paired t-test was utilized for analyses in (D) and (E). An unpaired t-test was employed for (F) and (G). The numbers inside the bars denote the number of cells in each group. Data are presented as mean ± SEM. Scale bars: 50 pA/10 ms.

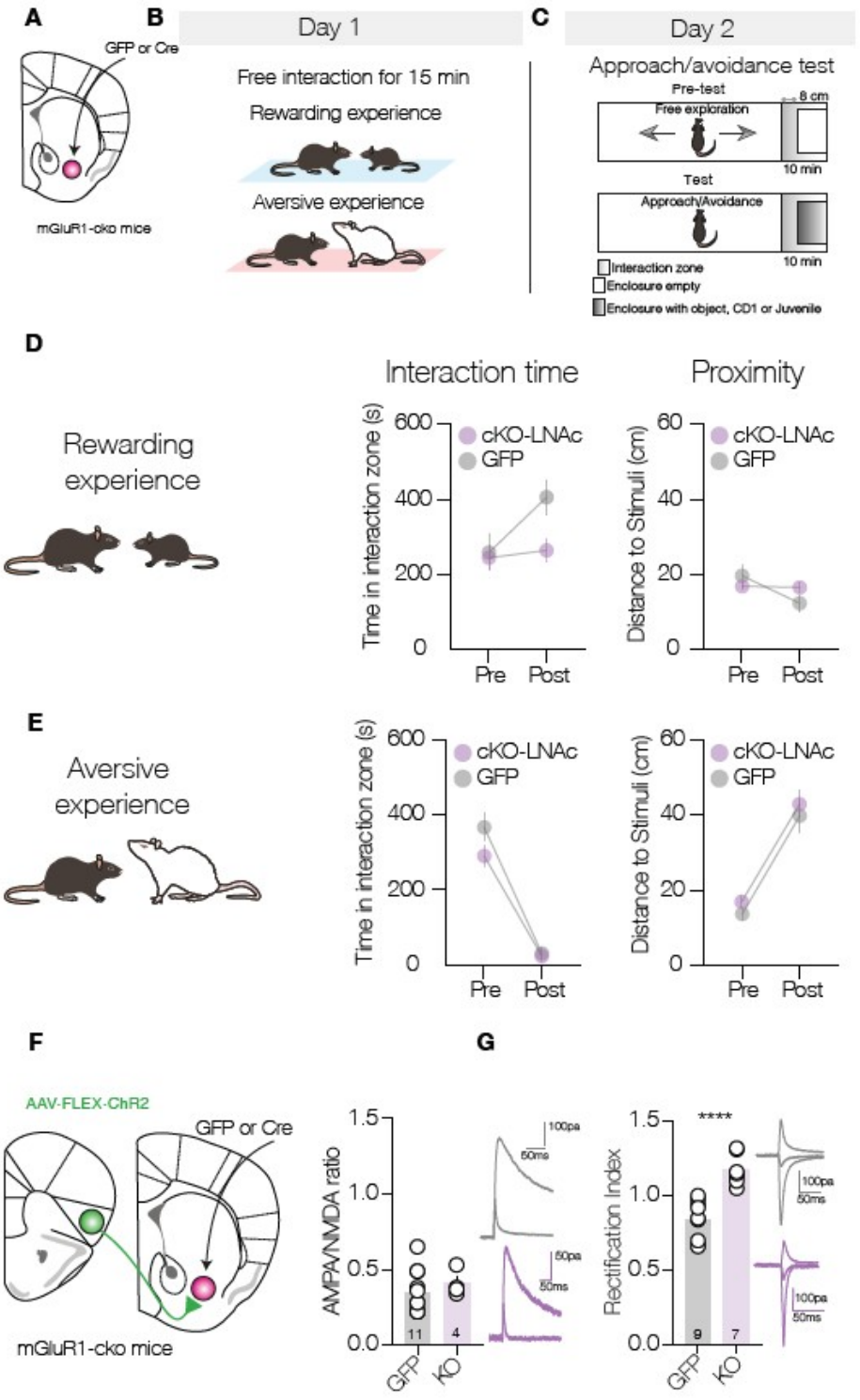


Figure 8

Positive social-valence plasticity requires mGluR1 signalling. (A) Viral strategy for conditional mGluR1 deletion: AAV-Cre was injected bilaterally into the LNAc of mGluR1cko mice to excise Grm1 locally (control animals received AAV-GFP). (B) Behavioural schematic. Day 1: 15-min free social interaction with a novel juvenile conspecific or CD-1 mouse. Day 2: 10-min habituation to an empty arena followed by 10 min with the previous stimuli in an enclosure (C). (D) Time in the interaction zone during the

rewarding paradigm. mGluR1-cKO mice failed to develop a preference. (E) Aversive experience. Both genotypes displayed robust avoidance of the CD-1 on Day 2, indicating intact learning of negative valence. (F) Synaptic consequences of ablation of mGluR1 in the LNAc: AAV-Cre in the LNAc of mGluR1cko mice combined with AAV-hSyn-ChR2-eYFP in the AIC. (G) Ex-vivo synaptic read-out. Left, AMPA/NMDA ratio; right, rectification index (RI). **** $p < 0.0001$ (t-test, non paired). Data are mean ± SEM. Scale bars and n for electrophysiology in each panel, behavior; n = 10 per group.

Supplementary Files

This is a list of supplementary files associated with this preprint. Click to download.

- NNA91523Figsuppcorrected17511071701.pdf